Structural analysis of a large span masonry arch bridge under railway loads

C. Molins, P. Roca and J. Casas
Technical University of Catalonia (UPC), Department of Civil Engineering, Barcelona, Spain

ABSTRACT: This paper presents the application of a numerical model specifically developed for the analysis of masonry constructions to the assessment of the capacity of a large open-spandrel masonry arch bridge nowadays in service subjected to railway loads. To appraise the behavior of these bridges the 85 m span structure erected over the Soča river at Solkan (Slovenia), just outside the town of Nova Gorica, on the border with Italy, was selected. Preliminary analyses were developed using a simplified axle load along the bridge. After that, Eurocode 1 railway live loads, both vertical and horizontal (braking or starting) loads had been considered. The paper discusses, based on the results achieved in this example, the behaviour and ultimate capacity of such structures, the convenience to take into account realistic distribution of loads when analyzing such structures at service and failure conditions and the influence of horizontal load.

1 INTRODUCTION

Most current methods for the assessment of masonry arches are oriented to the analysis of single arches and do not afford the study of more complex structures such as multi-arch bridges or open spandrel arches. In particular, methods based on limit analysis often require some drastic simplifications when applied to multi-span bridges, such as reducing the analysis to a single typical arch. All these simplifications are the result of the difficulty of foreseeing the position of the line of thrust (or the collapsing mechanism) in the case of complex structures including a set of arches and piers. In turn, the use of FEM approaches for the study of multi-arch bridges requires large scale, eventually prohibitive, computer effort. This is particularly the case when realistic, sophisticated constitutive equations for masonry are used.

Large masonry arches present always open spandrels because of the need to reduce the self weight and the transverse loading caused by flood water. Open spandrels allow, in particular, slender main arches and light foundations.

Only a few studies have been carried out on the load capacity of multi-span or open-spandrel arch bridges. Among these, the studies carried out on scale models by Melbourne et al. (1995), Prentice and Ponniah (1994) and Robinson et al. (1997), dealing with multi-arch bridges, and by Melbourne and Tao (1998), dealing with open-spandrel arch bridges, are to be mentioned.

Among the methods applicable to complex structures, the so-called Generalized Matrix Formulation (GMF) has been shown to provide an accurate and affordable numerical tool to assess multi-arch and open-spandrel arch bridges (Molins et al., 2001). This method, based on an extension of conventional matrix calculation to masonry structures, has been already presented with its application to the analysis of single arches and multi-arch bridges (Molins and Roca, 1998a). Other dimensional F.E. procedures have also successfully been applied to multi-arch bridges (Brencich and de Francesco, 2004).

In this paper, the capacity of the GMF method to deal with complex masonry bridge structures is further shown through its application to the analysis of multi-span or open-spandrel-arch masonry railway bridges. Taking advantage of the use of GMF, the authors assess the response of a large open-spandrel-arch masonry bridge, namely the one over the Soča river at Solkan (Slovenia), subjected to Eurocode 1 railway loads. A comparison is made of the results achieved by different configurations of the railway loads when analyzing large span masonry arches at service and, mainly, failure state.

2 THE GMF METHOD

As mentioned, the calculations presented in this paper were developed using an extension of conventional matrix calculation for the study of masonry spatial structures composed of curved, spatial members with variable cross section (Generalized Matrix Formulation or GMF). Nonlinear material behaviour is included by means of an elastoplastic constitutive equation for shear and compression, while a linear-elastic perfectly brittle response is assumed in tension. Nonlinear geometric effects caused by the imposition of the equilibrium condition upon the deformed configuration of the structure are considered, but assuming that the increments of both displacements and sectional rotations are moderately small.

In spite of using the smeared cracking approach, the method shows the capacity to describe highly concentrated damage and, thus, to indirectly simulate the generation of a number of hinges leading to instability. As shown in previous studies, the ultimate capacity of arches or general skeletal masonry constructions can be satisfactorily predicted. However, the stiffness of the structures after the generation of the hinges may be overestimated. More details of the formulation can be found in Molins and Roca (1998b).

The capacity of the method to analyze open spandrel arch bridges was formerly demonstrated through the simulation of the experimental results achieved by Melbourne and Tao (1998), on model spanning 5 m. The comparison of the numerical and experimental results was presented in Molins et al. (2001).

3 SOLKAN BRIDGE

3.1 Description of the bridge

This bridge crosses the Soča river near Solkan (Slovenia) just outside the town of Nova Gorica on the border with Italy. The railway bridge was built in 1905 as one of the key structures on the second railway line between Viena and Trieste, the Astro-Hungarian Empire's most important port. The Austrian State Railway company began constructing the bridge in the spring of 1903 according to the design of engineer Rudolf Jaussner. As Humar (2001) pointed out, the bridge over the Soča in Solkan is entirely constructed of worked stone and thus is the largest arch in Europe built of voussoirs. In fact, the arch at Solkan is 35 centimeters longer than the Adolphe Bridge in Luxemburg, designed by Paul Séjourné. The authors have presented results of the analysis of Adolphe bridge subjected to an axle load (Molins et al., 2001).

The original design of Solkan bridge was an 80 m arch, but finally it was increased to 85 m. Basic building material was shell limestone from the quarry at Nabresina near Trieste in Italy.

The actual state of Solkan bridge is the result of two main historic retrofitting works. The first one was due to the blowing up during a withdrawal of the Austrian army in the First World War. It was substituted by a steel truss during the same conflict. Later, the steel truss was substituted by the actual ashlar masonry arch. Figures 1 and 2 show drawings of the original design of the bridge, which has been used for the analyses presented in this paper. The main difference between the original and the present bridges are the number of the spandrel arches, which was reduced to four in the present one.

3.2 Geometry

The main arch spans 85.00 m and its rise at the crown is 21.80 m. It is symmetric with respect to the crown and the span of the spandrel arches is variable, decreasing towards the crown, as can be seen in Figure 2. Table 1 summarizes the main geometrical properties of the bridge.

The bridge presents three approaching arches on the Solkan riverside and six on the opposite one. As can be seen in Figure 1, all of them have different size. The overall length of the bridge, including the approaching arches, is 220 m.

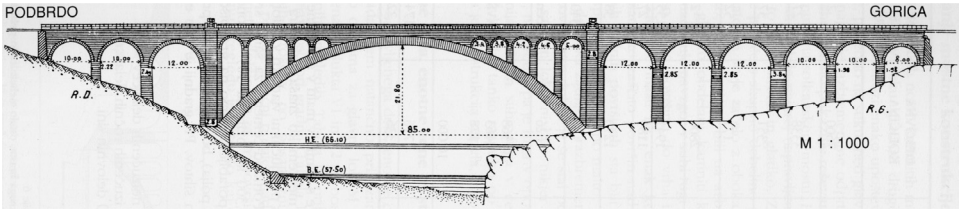

Figure 1 : Longitudinal section of Solkan Bridge (Humar, 1996).

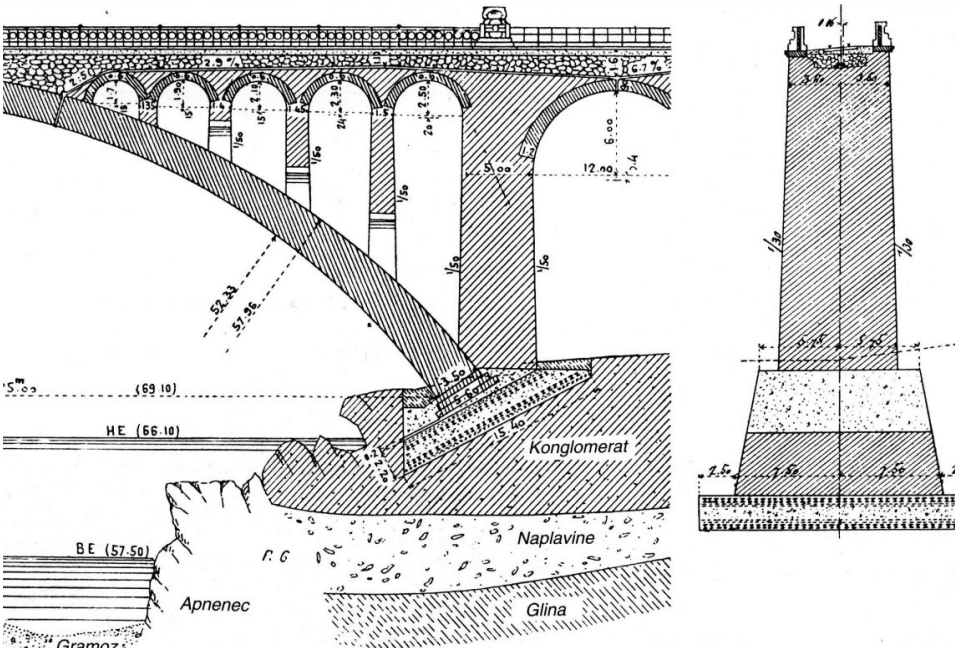

Figure 2 : Longitudinal section of the abutment of the main arch (Humar, 1996).

3.3 Model

The full bridge was modelled, including the main arch, the spandrel piers and arches and the approaching piers and arches (Figure 3). The final model was composed of 256 nodes and 113 GMF elements. Fourteen FMG elements were used to model the main arch and only four were used in each spandrel arch (Figure 4). All piers were modelled by one element but the ones on the abutments of the main arch and the others which sustain arches at different heights.

3.4 Materials

Average material properties of the fabric (Table 2) were estimated by empirical formulae from information on the component materials provided by Humar (1996) and by authtors' experience.

Table 1 : Geometrical properties of the bridge.

MAIN ARCH	
Shape	Segmental
Free span	85.00 m
Arch thickness	2.10-3.60 m
Arch width	7.20 m
Rise at mid-span	21.80 m
Width of main piers	5.00 m
SPANDREL ARCHES	
Shape	Circular
Span of spandrel arches	3.40-5.00 m
Arch thickness	0.60 m
Height of spandrel pier	1.60-11.65 m
Width of spandrel pier	1.30-1.50 m
APPROACHING ARCHES	
Shape	Circular
Span of spandrel arches	8.00-10.00-12.00 m
Arch thickness	0.90 m
Width of piers	1.98-3.80 m

Figure 3 : Complete model of the bridge.

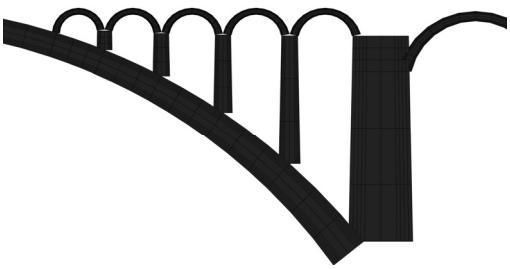

Figure 4 : Model of the abutment of the main arch.

3.5 Loading

Dead loads (DL) and live loads (LL) produced by trains on the structure have been considered. LL includes the weight of trains and tangential forces due to braking and starting. In addition, the combined effect of railway LL and wind was analyzed. The vertical loads considered were: (a) one axle along the bridge (as a reference), (b) 4 axle of 250 kN each (SET 1), according to the locomotive weight considered in Eurocode 1, (c) the latter axle plus 5 m of uniform 80 kN/m loading (SET 2), (d) the 4 axle plus 20 m of uniform 80 kN/m loading (SET 3), (d) SET 2 plus tangential starting load: 31 kN/m uniformly distributed along the train; and (f) SET 3 plus

tangential starting load. The loading schemes are shown in Figure 5. Figure 6 shows the fourteen different positions of the axis of the set of 4 axle loads analyzed in this work.

Table 2 : Material properties of the bridge.

MAIN ARCH	
Deformational modulus	12000 N/mm^2
Compressive strength	25.0 N/mm^2
Tensile strength	0.01 N/mm^2
Unit weight	24.0 kN/m^3
APPROACHING AND SPANDREL ARCHES	
Deformational modulus	10000-7000 N/mm^2
Compressive strength	25.0 N/mm^2
Tensile strength	0.01 N/mm^2
Unit weight	20.0 kN/m^3

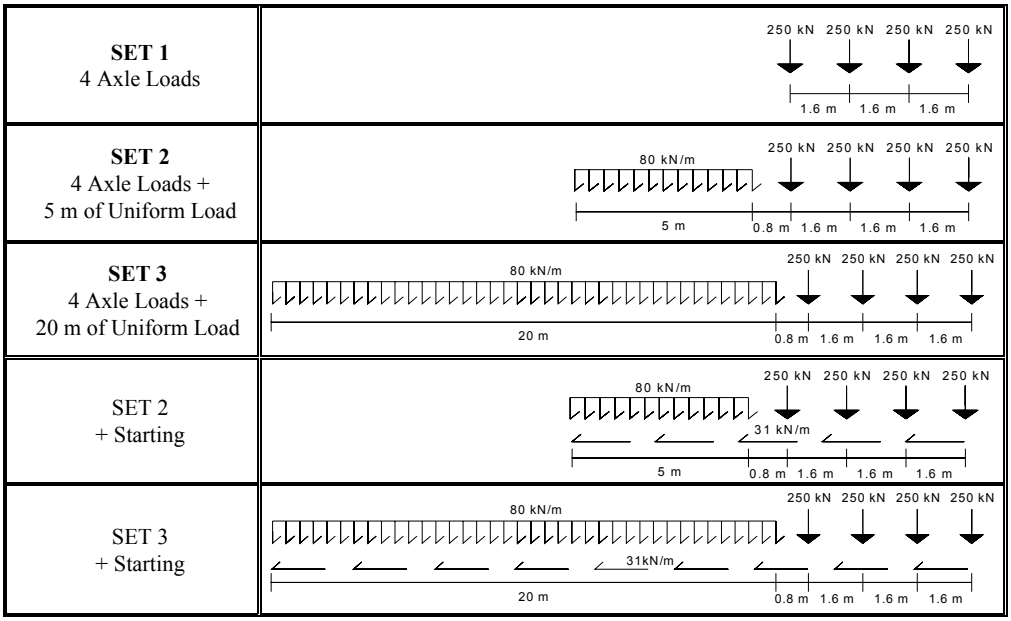

Figure 5 : Railway load patterns used in the analyses.

4 RESULTS

Under DL the main arch is almost uniformly compressed. The largest numerical deflection under DL is reached at L/4 and its value is 20.1 mm. It also causes significant cracking in the spandrel arches due to the deflection of the main arch. However, this result is not realistic because spandrel arches were always built after the main arch was erected.

When subjected to an axle LL along the main arch (excluding spandrel arches), the worst position was attained at 0.26 L (where L is the free span of the main arch), on the shortest spandrel pier, as can be shown in Figure 7 and Table 3. Failure was produced by achieving the ultimate strain in compression in the extrados of the main arch in the loaded section, without completing the four hinges mechanism. After that preliminary analysis, the set of four axle (SET 1) was applied on the fourteen selected positions. The lowest load resisted by the bridge was 6.35 MN at 0.08 L (P2), on the highest spandrel pier. It corresponds to a load factor (LF) of 6.35. The mechanism was a local one involving three-hinged spandrel arches and tilting of the second

spandrel pier. When acting on the crown of the spandrel arches, the ultimate load was higher than in the case of acting aligned on the piers.

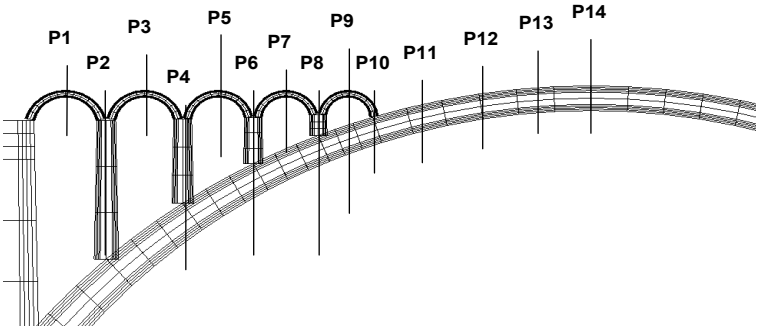

Figure 6 : Position of the barycentre of the axle loads on the main span.

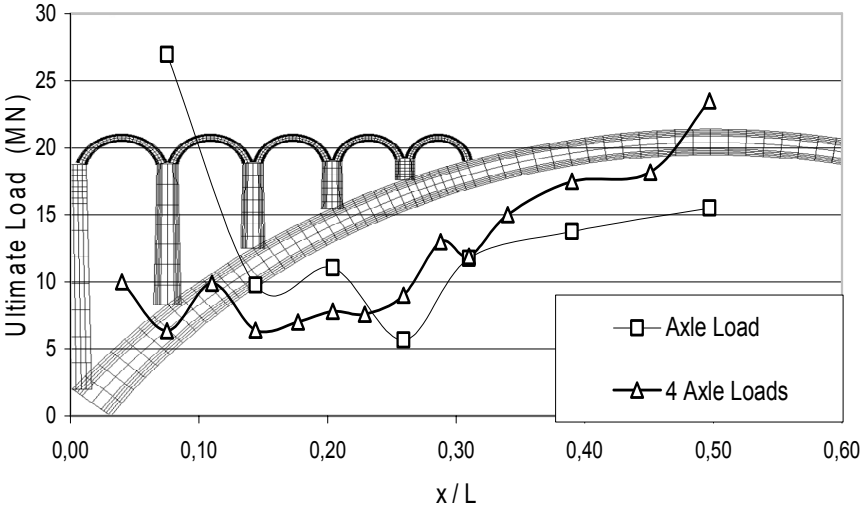

Figure 7 : Influence of the loads position on the ultimate capacity, for one axle or four axle loads.

Table 3 : Failure loads (MN).

x/L	Axle Load	4 Axle Loads
0,04		10,00
0,08	26,95	6,35
0,11		9,90
0,14	9,75	6,40
0,18		7,00
0,20	11,05	7,80
0,23		7,60
0,26	5,67	9,00
0,29		13,00
0,31	11,75	11,90
0,34		15,00
0,39	13,75	17,50
0,45		18,17
0,50	15,50	23,50

As Fig. 8 shows, failure is reached before completing a five-hinges mechanism because ultimate strain of masonry in compression is attained at the crown.

Figure 9 shows a comparison of the failure loads for loading sets 1 to 3 in terms of applied load and of load factor. Table 4 also shows the numerical results corresponding to Fig. 9 and the effect of including tangential starting forces.

As can be understood from Figure 9 and Table 4, the weakest part of the bridge under vertical live loads is the open spandrel. The lowest Load Factor is 2.70 and is attained at 0.20 L for the set 2 load. However, all load factors between 0.20 and 0.29 L are below 4.2 for the sets 2 and 3. On the contrary, minimum ultimate total load for the set 3 (7.80 MN) in that critical zone is higher than for the set 2 (3.78 MN). As could be expected, the capacity of the arch is larger when subjected to more spread loads than to concentrated loads.

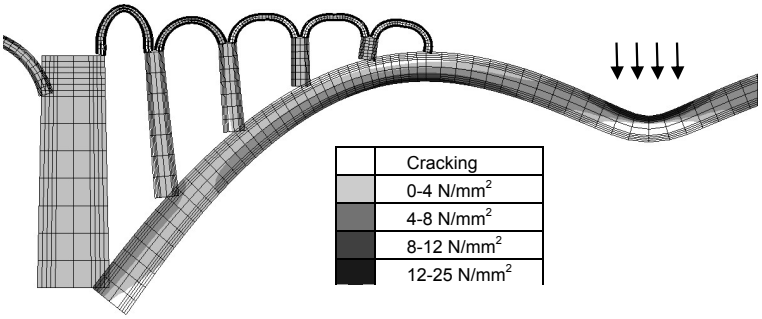

Figure 8 : Stress state and deformation (x100) of the arch subjected to a 4 axle load at mid span at failure.

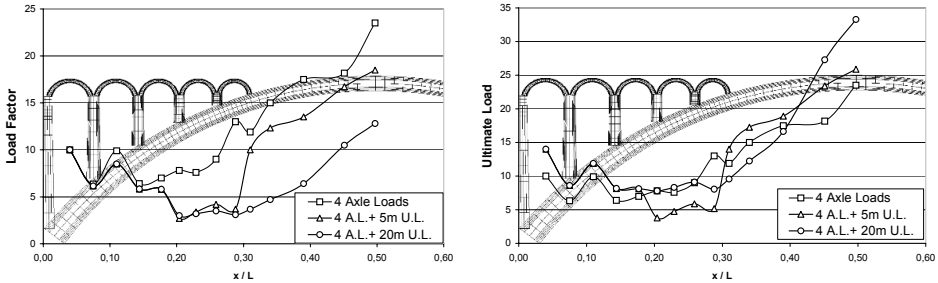

Figure 9 : Comparison of Load Factor (a) and Ultimate Load (b) for different loading sets.

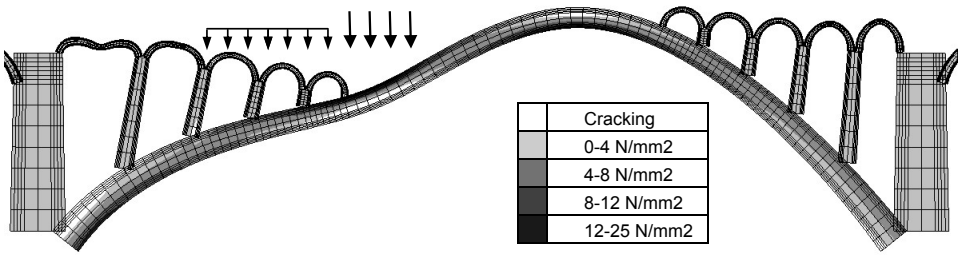

Figure 10 : Stress state and deformation (x50) of the arch subjected to a 4 axle plus 20 m of uniform load.

Simultaneous action of railway weights and starting does not significantly affect the minimum values of the load factors. However, for loading SET 3, it can be observed that load factors of the positions on the piers increase while LF on the crown of spandrel arches decrease when tangential loads are included. The inclusion of characteristic wind loads in combination with railway vertical loads almost not affected the ultimate capacity of the bridge.

Table 4 : Results with and without the inclusion of the tangential forces due to starting.

	SET 2		SET 3		SET 2 + START		SET 3 + START	
x/L	L. F.	U. L.	L. F.	U. L.	L. F.	U. L.	L. F.	U. L.
0,04	10,00	14,00	10,00	14,00	9,10	12,74	9,10	12,74
0,08	6,14	8,60	6,14	8,60	8,47	11,86	8,47	11,86
0,11	8,50	11,90	8,50	11,90	8,40	11,76	8,40	11,76
0,14	5,83	8,16	5,83	8,16	5,40	7,56	5,40	7,56
0,18	5,80	8,12	5,80	8,12	5,10	7,14	5,10	7,14
0,20	2,70	3,78	3,00	7,80	2,70	3,78	5,00	13,00
0,23	3,40	4,76	3,20	8,32	4,10	5,74	2,70	7,02
0,26	4,20	5,88	3,50	9,10	3,90	5,46	5,10	13,26
0,29	3,70	5,18	3,10	8,06	6,67	9,34	3,00	7,80
0,31	10,00	14,00	3,68	9,57	8,80	12,32	2,90	7,54
0,34	12,33	17,26	4,71	12,25	15,70	21,98	7,57	19,68
0,39	13,50	18,90	6,40	16,64	15,08	21,11	8,00	20,80
0,45	16,71	23,39	10,50	27,30	20,10	28,14	10,43	27,12
0,50	18,50	25,90	12,80	33,28	16,50	23,10	16,10	41,86

L.F= Load Factor, U.L=Ultimate Load (MN).

5 CONCLUSIONS

The ultimate capacity of a large span masonry arch subjected to design railway loads, including different patterns of live loads, starting and braking forces and wind action, has been analyzed using the GMF method. The analysis has confirmed the applicability of this numerical approach to the analysis of complex and large masonry arch bridge structures.

Moreover, the analysis has permitted the identification of meaningful aspects regarding the response of multi-arch bridges with open spandrels subject to railway loads. In the case of the bridge over the Soča, the method has afforded the determination of the worst loading patterns and their critical position have been found. The worst situation is attained by set 2 (four 250 kN axle plus 5 m of 80 kN/m) acting at one fifth of the span. Ultimate loads experience slight changes when tangential forces due to starting are included.

ACKNOWLEDGMENTS

The authors want to acknowledge the financial support provided by the European Commission (VI Framework Program, SUSTAINABLE BRIDGES: TIP3-CT-2003-001653).

REFERENCES

Brencich, A. and De Francesco, U. 2004. Assessment of multispan masonry arch bridges. I: Simplified approach. *Journal of Bridge Engineering*, v 9, n 6, p 582-590.

Humar, G., 1996. *Kamniti velikan na Soči*, Nova Gorica: BRANKO d.d.o.

Humar, G. 2001. World famous arch bridges in Slovenia. *Arch'01. Third international arch bridges conference. Paris 19-21 sept 2001.* p. 121-126. Paris: Presses de l'école nationale des Ponts et chaussées.

Melbourne, C., Gilbert, M. and Wagstaff, M. 1995. The behaviour of multi-span masonry arch bridges. *Proc. 1st int. conference arch bridges*. London: Thomas Telford.

Melbourne, C. and Tao, H. 1998. The behaviour of open spandrel brickwork arch bridges. *Arch bridges, Proceedings of the 2nd international conference on arch bridges.* Rotterdam: A. A. Balkema.

Molins, C. and Roca, P. 1998. Load capacity of multi-arch masonry bridges. *Arch Bridges*. *Proceedings of the 2nd international conference on arch bridges.* Rotterdam: A. A. Balkema.

Molins, C. and Roca, C. 1998. Capacity of masonry arches and spatial structures, *Journal of Structural Engineering ASCE*, v 124, n 6 p. 653-663.

Molins, C., Roca, P. and Pujol, A. 2001. Numerical simulation of the structural behaviour of single, multi-arch and open-sprandel arch masonry bridges. *Arch'01. Third international arch bridges conference. Paris 19-21 september 2001.* p. 523-530. Paris: Presses de l'école des ponts et chaussées.

Prentice, D.J. and Ponniah, D.A. 1994. Testing of multi-span model masonry arch bridges. *Proc. centenary year bridge conference*, Cardiff, Elsevier Science, p.169-174.

Robinson, J.I., Ponniah, D.A., & Prentice, D.J. 1997. Soil pressure measurements on a multi-span brick arch. *Proc.7th int. conf. on structural faults and repair*, Eng. Technics Press, Edinburgh. p. 111-119.